Letters in Applied NanoBioScience
Open-Access Journal (ISSN: 2284-6808)

Review
Volume 13, Issue 3, 2024, 107
https://doi.org/10.33263/LIANBS133.107

Molecular Structural Aspects, Stability, Bonding and Spectroscopic Properties in Sn(IV) Porphyrin Compounds – A Theoretical Investigation

Rajesh R [1], Dileep D [1], Brindha Veerappan [2], Sivasankar B N [1], Krishnamoorthy Bellie Sundaram [2,*]

[1] Department of Chemistry, Government Arts College, Udhagamandalam, The Nilgiris, Tamil Nadu, India, 643 002;
[2] Department of Chemistry SF, PSG College of Arts and Science, Coimbatore, Tamil Nadu, India, 641014; Rajeshrtejas@gmail.com (RR); ddileep1982@gmail.com (DD); vbrindhaveerappan@gmail.com (VB); sivabickol@yahoo.com (SBN); bskimo@yahoo.co.in (BSK);
* Correspondence: bskimo@yahoo.co.in (B.S.K);

Scopus Author ID 57197658621

Received: 25.05.2023; Accepted: 30.12.2023; Published: 25.07.2024

Abstract: Porphyrin is an important molecule with diverse applications. Similarly, tin compounds are important with applications ranging from industries to biological fields. When tin forms a complex with porphyrin, the resulting hybrid complex is expected to show diverse structural features with potential applications. In fact, tetraethyl phorpyrinatotin is water soluble and possesses anti-cancer activity. Here, we have studied the electronic and geometric structural features and spectroscopic properties of the different tin(IV)porphyrins of the type **[SnPX$_2$]** where **P** = porphyrin; **X** = **F (1)**, **Cl (2), Br (3)**, **I (4)** were optimized using the DFT method at BP86/TZVP level. The DFT computed molecular geometries, ^{1}H, ^{13}C, and ^{119}Sn nuclear magnetic resonance (NMR) spectroscopy chemical shift values and reactive descriptors are in good agreement with experimentally known or related molecules.

Keywords: porphyrin; DFT; tin(IV); NMR; molecular orbital.

1. Introduction

Tin is an essential element known to humans well before and exhibits diverse structural features. Being an important part of photosynthesis, porphyrin moiety exhibits diverse applications. Tin-Porphyrins are hybrid complexes consisting of both tin substrate and porphyrin ring. An excellent review on tin porphyrins covering the years before 2004 is provided by D. P. Arnold. [1-3]. These tin porphyrins show a wide range of applications, from catalysis, biological activities like photodynamic therapy (PDT) for the treatment of cancer and even for AIDS, material chemistry, catalytic and photocatalytic activities including the splitting of water to produce hydrogen, DNA binding ability for cancer research and gene technology, treatment of neonatal hyperbilirubinemia, etc. [4-8]. Tin(IV) porphyrins are known to be more stable than tin(II) porphyrins [9]. Tin (II) porphyrins easily and quickly undergo oxidative addition in solution and air to form tin(IV) porphyrins. The tin(IV) porphyrin complexes can be readily prepared and are stable enough under acidic conditions. The geometry around these six-coordinate Sn(IV) compounds is octahedral with two *trans*-axial ligands. Different anions are substituted in these trans-axial positions for new tin(IV) porphyrin derivatives. Tin(IV) porphyrin derivatives containing more than one porphyrin ring can also be synthesized due to the exophilic nature of the tin center [1]. The spectral and electrochemical properties of various

Sn(IV) were studied, and their studies showed that the properties are sensitive to the nature of substituent present at the meso-position [10]. The β-brominated tin(IV) porphyrins are found to be used as potential photosensitizers for medical and energy applications [11]. Only very few computational studies are known for tin porphyrin compounds. Recent studies show that tin porphyrins can act as molecular electrocatalysts for proton reduction reactions [5]. Chloro-substituted Tin(IV) porphyrin SnTPPC is an example of an effective photosensitizer during photocatalytic proton reduction, which in turn proceeds through two mechanisms: reductive mechanism and oxidative quenching mechanism [12]. Tin-porphyrin complexes are also known for life-forming molecules like amino acids, especially with L-proline [13]. Though there are many experimental studies and biological applications of tin porphyrin compounds, theoretical studies to investigate their behavior at the molecular level are scarce. Time-dependent density functional theory calculations have been employed to characterize the inter-macrocycle interactions introduced when two tin(IV) porphyrins are axially covalently bonded *via* an ethynyl linker, which can be used in a solar light harvesting system [14]. Density functional theory (DFT) calculations are used to predict the atomic structure and dynamics [15] accurately.

Human aging and many diseases are mainly related to oxidative stress. Superoxide dismutase (SOD) mimicking artificial enzymes has been the star of anti-oxidation in recent years. Among the different metalloporphyrins engineered to act as novel SOC-mimics, Sn-porphyrins (Sn-TCPP) succeed in flowing (unusually highly catalytic activity) towards catalyzing the disproportionation of superoxide radicals ($\cdot O_2^-$) anions due to H_2O_2 and O_2. This is due to the Sn(IV)/Sn(II) transition at (Sn-TCPP) *meso*-tetra(4-carboxy phenyl)porphine. This shows the way Sn porphyrin-based nano enzymes would be a potent alternative for natural SODs [16]. Tin-porphyrins have also proven to be successful in the chemoprevention of neonatal jaundice, i.e., the prevention of neonatal hyperbilirubinemia [17].

As the green chemistry techniques are highly receiving attention from the research community, environmentally benign techniques are used to synthesize tetra(4-methylpyridiniumyl) and tetra (4-pyridyl)porphyrinato Sn(IV) complexes and the 4-methylpyridinimyl derivative is water soluble and tetra(4-pyridyl) derivative is water insoluble. This reaction proceeds with water as a solvent at room temperature [18]. Sn-porphyrins treated with polyethylene glycol (PEG) form hydrogel polymers, which are highly important due to pH-responsive fluorescence [19].

Computational chemistry tools like DFT methods are being successfully used to study the structural features of biologically important molecules at the molecular level. Here, we have studied the electronic, geometric structural features and spectroscopic properties of the different tin(IV)porphyrins of the type [$SnPX_2$] where P = porphin; X = F (1), Cl (2), Br (3), I (4) were optimized using the DFT method at BP86/TZVP level, to get the more stable products with diverse applications.

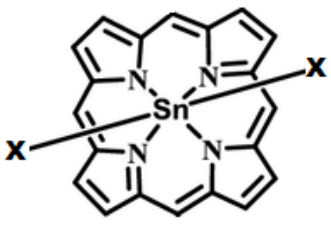

Scheme 1. Schematic representation of the molecules studied [$SnPX_2$] where P = porphyrin; X = F (1), Cl (2), Br (3), I (4).

2. Computational Details

Computational chemistry has been used to characterize newly designed compounds and already reported compounds lacking complete structural characterization [20]. All the Density Functional Theory calculations were carried out using the ORCA program developed by F. Neese and co-workers [21]. The Vosko-Wilk-Nusair parameterization was used for the local density approximation (LDA) with gradient corrections for exchange (Becke88) and correlation (Perdew86) [22-25]. TZVP (triple zeta valance with polarization function) basis set was used for all the molecules. In all the calculations, TightSCF convergence criteria were used [26]. Optimized geometries were checked using the following frequency calculations in order to ensure that the obtained geometry is the minimum [27, 28]. Further, the DFT-optimized geometries were used to calculate the NMR parameters like shielding constants, chemical shifts, etc., with the help of the EPRNMR module, which is available in the ORCA software [29]. Tetramethylsilane (TMS) was used as a reference for the calculation of ^{1}H and ^{13}C NMR chemical shift values, whereas tetramethyltin was used as a reference for the ^{119}Sn NMR chemical shifts [30, 31]. The reactivity descriptors like chemical potential (μ), hardness (η), softness (S), and electrophilicity (ω) are computed using the HOMO and LUMO energies with the following expressions. Chemical potential (μ) = $E_{LUMO + HOMO}/2$; Hardness (η) = $E_{LUMO - HOMO}/2$; Softness (S) = 1/ η; Electrophilicity (ω) = $\mu^2/2\eta$; The DFT computed global reactivity descriptors are already proved to be successful in predicting the reactivities of the compounds studied and being used to describe the reactive sites of these important clusters [32].

3. Results and Discussion

Porphyrins and metalloporphyrins are important molecular units that play a vital role in the life cycle. Tin porphyrins are important molecules having potential applications in different fields, viz., photodynamic therapy (PDT) for the treatment of cancer and even for AIDS [9, 10], catalytic and photocatalytic activities, including the splitting of water to produce hydrogen[33], DNA binding ability for cancer research and gene technology and other biological applications[34], treatment of neonatal hyperbilirubinemia[35, 36], etc. Though there are many experimental studies with material and biological applications of tin porphyrins, theoretical studies to investigate their behavior at the molecular level are scarce. Computational tools are being practiced by chemists to address the complete study of the existing reactions, modeling the new compounds, and designing new routes for synthesizing new compounds. The interesting results obtained from the DFT calculations on the geometrical structure, electronic structure, bonding analysis, and thermal stability of the tin(IV)porphyrins of the type $SnPX_2$ [where P = porphyrin; X = F (1), Cl (2), Br (3), I (4)] from our computations are discussed below.

3.1. Geometrical structure.

The DFT-optimized geometries at BP86/TZVP level for the tin(IV)porphyrins $SnPF_2$ (1), $SnPCl_2$ (2), $SnPBr_2$ (3), and $SnPI_2$ (4) studied are provided in Figure 1. The DFT-optimized metrical parameters like bond lengths and bond angles are provided in Table 1. The synthesis and characterization of tin(IV)porphyrins with halogen ligands is an important area of tin porphyrin chemistry. Since tin, in nature, can form a variety of compounds using reductive elimination, these compounds can be used in many fields, especially in developing metal-organic frameworks. The DFT-optimized geometries of $SnPF_2$ (1), $SnPCl_2$ (2), $SnPBr_2$ (3), and

$SnPI_2$ (4) resulted in octahedral geometry as expected, and the nitrogen atoms occupy equatorial positions. The halogen atoms in these molecules occupy the axial positions. The tin atom lies in the middle of the porphyrin plane and connects the four nitrogen atoms of the porphyrin and two oxygen atoms of the halogen atoms. The DFT computed bond parameters for the compounds $SnPF_2$ (1), $SnPCl_2$ (2), $SnPBr_2$ (3), and $SnPI_2$ (4) are in good agreement with those of the experimental values obtained from X-ray crystallography. The DFT-computed values are given in Tables 1 to 4. The DFT computed Sn-N bond distance of 2.13 Å for nitrogen atoms in all the compounds is very close to the experimental values of the 2.06 Å obtained for the tetraphenyl derivative. The DFT-computed Sn-Halogen bond lengths in compounds 1-4 also agree with the experimental values for similar compounds. The tinchloride-porphyrin complex, when mixed with poly(3-hydroxybutyrate), which is an electrospun ultrathin fiber, enhances the properties of the polymeric fiber [37].

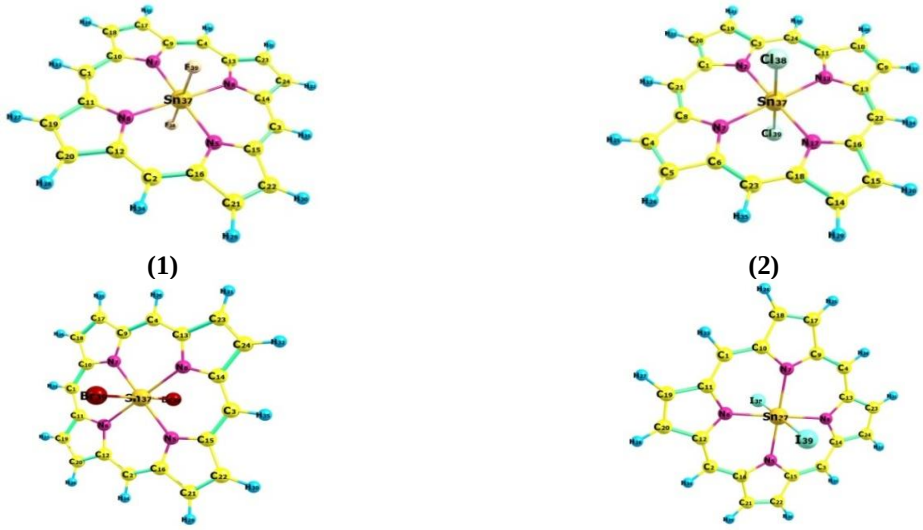

Figure 1. DFT (BP86/TZVP) Optimized Geometry for the compound **(1)** $SnPF_2$; **(2)** $SnPCl_2$; **(3)** $SnPBr_2$; **(4)** $SnPI_2$.

3.2. Bonding and stability.

The DFT computed energies of the HOMO, LUMO, and the energy gap $E_{LUMO-HOMO}$ are listed in **Table 3**. The DFT computed energy gap $E_{LUMO-HOMO}$ value of 2.0 eV for **$SnPF_2$ (1) c**onfirms the more stable nature of compound **(1)** when compared to that of chloro, bromo, and iodo compound **(2-4)**. The DFT computed $E_{LUMO-HOMO}$ values confirm the stability of compound **1** at room temperature and the formation of clusters **2, 3,** and **4** at low temperatures, suggesting their possible formation in the laboratories—the frontier molecular orbital of the compounds studied at DFT level.

Table 1. DFT computed metrical parameters of the compounds $SnPF_2$ **(1)**, $SnPCl_2$ **(2)**, $SnPBr_2$ **(3),** and $SnPI_2$ **(4),** and the experimental values of tetraphenyl derivative are in square brackets.

Atoms		**Sn37 –N5**	**Sn37 – N6**	**Sn37 – N7**	**Sn37 – N8**	**Sn37 – X38**	**Sn37 – X39**
Bond Length (Å)	**1**	2.129 [2.064]	2.129 [2.064]	2.129 [2.064]	2.129 [2.064]	2.016 [1.964]	2.016 [1.964]
	2	2.130	2.130	2.130	2.130	2.477	2.482
	3	2.132	2.132	2.132	2.132	2.646	2.646
	4	2.133	2.133	2.133	2.133	2.891	2.891
Atoms		**N5–Sn37–N6**	**N7–Sn37–N8**	**N5–Sn37–X39**	**N6–Sn37–X39**	**N7–Sn37–X38**	**N8–Sn37–X39**
Bond Angle (°)	**1**	90.00	90.00	90.00	90.00	90.00	90.00
	2	90.02	89.99	90.09	89.94	89.91	90.05
	3	90.00	90.00	90.00	90.00	89.99	90.00
	4	90.00	90.00	90.00	90.00	90.00	90.00

The Mayer bond analysis (MBA) describes the number of bonds and the various types of bonds present between two atoms, as shown in Table 2. The Sn-N bond orders are ranging from 0.39 to 0.69. The strong Sn-N bonding interaction is exhibited by compound (2) with a bond order value of 0.69, followed by compound (1) with a bond order of 0.42. Compounds (3) and (4) also show considerable Sn-N bonding with bond order 0.40. The Sn-halogen (X) bond orders are ranging from 0.70 to 1.36. The bond order between the Sn-I is 1.36 in (4), which shows the strongest interaction among the four with 2.89 Å bond length, followed by a Sn-Br bond order of 1.17 in (3). The bond strength gradually increases from F to I (F < Cl < Br < I). This proves that the nature of the Sn-X depends on the electronegativities of the halogen atoms.

Table 2. DFT computed Mayer bond order (MBO) analysis of the compounds $SnPF_2$ **(1)**, $SnPCl_2$ **(2)**, $SnPBr_2$ **(3),** and $SnPI_2$ **(4)**.

S.No	Sn37 –N5	Sn37 – N6	Sn37 – N7	Sn37 – N8	Sn37 – X38	Sn37 – X39
1	0.4239	0.4242	0.4235	0.4250	0.7075	0.7078
2	0.6948	0.6948	0.6944	0.6957	0.9342	0.9344
3	0.3968	0.3974	0.3965	0.3974	1.1738	1.1739
4	0.3978	0.3983	0.3975	0.3984	1.3678	1.3679

The above details prove that the 'N' atoms from the porphyrins are more closely attached to the central metal atom 'Sn' than the halogens (F, Cl, Br, I).

3.3. Electronic structure.

By using Koopmann's theorem, DFT calculations were made to calculate the electronic properties of the tin(IV)porphyrins, like ionization potential, electron affinity, absolute hardness, chemical potential, and electrophilicity. The values of HOMO and LUMO energies are displayed in Table 3. Ionization potential is the negative of the HOMO energy value, and electronic affinity is the negative of the LUMO energy value. The high value of HOMO shows the electron-donating ability of an appropriate molecule of the low empty molecular orbital. The DFT computed E_{HOMO} values of -5.5 to -3.6 V show the highest electron donating ability for 1-4. The LUMO-HOMO energy gap is an important parameter as a function of the reactivity of the clusters. The $E_{LUMO-HOMO}$ increases, and the reactivity of the molecule decreases. The low value of $E_{LUMO-HOMO}$ suggests the reactive nature of the compound (4). From the $E_{LUMO-HOMO}$ values, the increasing reactivity of the compounds is in the order 1 < 2 < 3 < 4. The hardness values are the index of stability of the molecule, and the DFT computed hardness values suggest stability increase in the order 1 > 2 > 3 > 4 for the tin(IV)porphyrins studied. Hardness values also confirm the more stable nature of the tin(IV)porphyrin (1).

Table 3. DFT computed $E_{LUMO-HOMO}$ energies (eV), chemical potential, hardness, softness, electrophilicity, ionization potential, and electron affinity for the compounds $SnPF_2$ **(1)**, $SnPCl_2$ **(2)**, $SnPBr_2$ **(3)** and $SnPI_2$ **(4)**.

Compound	1	2	3	4
HOMO	-5.5358	-5.5495	-5.5428	-5.3596
LUMO	-3.5764	-3.6621	-3.6951	-3.7473
$E_{LUMO-HOMO}$	1.9594	1.8874	1.8477	1.6123
Chemical potential (μ)	-4.5561	-4.6058	-4.6189	-4.5534
Hardness (Ƞ)	0.9797	0.9437	0.9238	0.8061
Softness (S)	1.0238	1.0596	1.0824	1.2405
Electrophilicity (Ꞷ)	10.5940	10.0094	11.5469	12.8603
Ionization potential (eV)	5.5358	5.5495	5.5428	5.3596
Electron Affinity (eV)	3.5764	3.6621	3.6951	3.7473

The DFT computed electrophilicity (ω) values suggest the most electrophilic nature for the compounds ranging from 12.7 eV (4) to 10.0 eV (2).The FMO pictures are shown in Figure 2. The HOMO of the molecules is mainly from the porphyrin ring in the case of $SnPF_2$ (1), $SnPCl_2$ (2), and $SnPBr_2$ (3), but the HOMO of the compound $SnPI_2$ (4) is mainly from the unpaired electrons of iodine. HOMO-1 orbital of compound (3) also mainly comes from the unpaired electrons of bromine. Thus the different arrangements of the HOMO and HOMO-1 orbitals for the compounds 1-4 lead to the different reactivity of these compounds towards other reagents. Tin orbitals are not involved in the HOMO, LUMO, HOMO-1, and LUMO+1 of compounds 1-4. In the HOMO-1 orbitals, a significant contribution is from the porphyrin ring in compounds 1 and 2. Meanwhile, there is a significant contribution from halogen atoms, viz., bromine and iodine, in compounds 3 and 4.

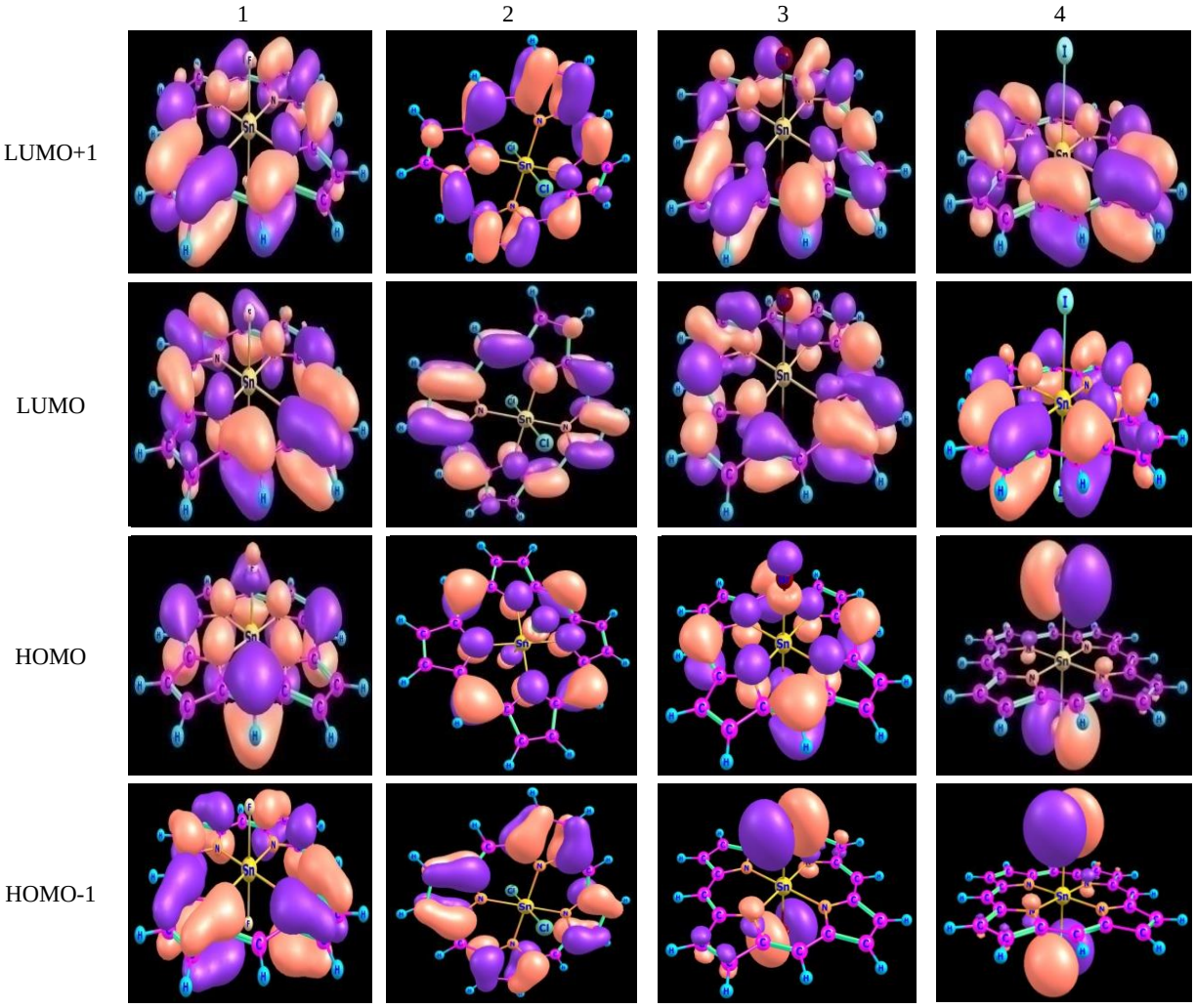

Figure 2. Frontiers molecular orbitals (FMO) obtained from DFT (BP86/TZVP) calculations for the compound (1) $SnPF_2$; (2) $SnPCl_2$; (3) $SnPBr_2$; (4) $SnPI_2$.

3.4. NMR spectroscopic properties.

Computational chemistry tools like DFT methods are being routinely used by chemists to aid their experimental findings. DFT calculations have already proved to be successful in calculating the shielding constants, chemical shifts, and contributions from paramagnetic and diamagnetic parts towards the total magnetic properties of the molecules. Here, we have computed the ^{1}H, ^{13}C, and ^{119}sn NMR chemical shift values for the compounds and compared them with the standard experimental values of the similar compound tetraphenylporphyrin Table 4. The DFT (BP86/TZVP) computed ^{1}H NMR chemical shift values are close to those

of the experimental values of the tetraphenyl derivative. Though the value for beta H of compound **2** is not available for the tetraphenyl derivative, it resonates around +9.4 ppm, which is closer to the values (9.14 ppm) obtained for a similar compound [38]. The DFT computed ^{13}C NMR values are in close agreement with those of the experimentally observed ^{13}C NMR chemical shift values of the tetraphenyl derivative. The three different types of carbon atoms in the porphyrin ring resonate around 111.31 ppm, 153.56 ppm, and 139.52 ppm, which are all closer to the experimental values.

Table 4. DFT computed ^{1}H, ^{13}C, and ^{119}Sn NMR chemical shifts (δ) for the molecule $SnPCl_2$ **(2)**.

S. No.	Type of Atoms	Chemical Shift (δ *ppm*)	
		DFT	Exp.*
^{1}H	*β* H	9.365	Ua
	meso H	10.288	9.24
^{13}C	C1	111.31	Ua
	C2	153.559	Ua
	C3	139.518	Ua
^{119}Sn	Sn	-58.716	Ua

*Exp. Values corresponding to tetraphenyl derivative.

Spectroscopy plays an important role in the understanding of the mechanisms of metalloporphyrins. Tin porphyrins as molecular catalysts for artificial photosynthesis [39] have also been reported. The formation of graphene oxide-linked tin(IV)porphyrins is also synthesized and confirmed through NMR spectra, which plays an important role in catalysis[40]. The DFT computed the ^{119}Sn NMR chemical shifts for the compound **(2)** are provided in Table 4. The DFT (BP86/TZVP) computed ^{119}Sn NMR chemical shift value of -58.7 ppm is lower when compared to that of the tetraphenyl derivative, though it is not advisable to compare. But the signal at upfield is in agreement with our expectations. DFT also predicts the reasonable chemical shift values for the compounds that are not available experimentally, but they can be compared with similar-type compounds, which can aid some ideas in understanding that molecule.

4. Conclusions

The tin(IV)porphyrins $SnPF_2$ (1), $SnPCl_2$ (2), $SnPBr_2$ (3), and $SnPI_2$ (4) are studied by using the DFT (BP86/TZVP) methods to get more insight into their molecular structural features. From the theoretical investigation, the following conclusions are made.

The DFT (BP86/TZVP) optimized molecular structures result in minima in the potential energy surface, and the bond parameters are in agreement with those of a similar compound with tetraphenylporphyrinato derivative.

The HOMO, LUMO energies, and the $E_{LUMO-HOMO}$ computed by the DFT method at BP86/TZVP level confirm the possible existence and the stability of the modeled tin(IV)porphyrin dihalides **1-4**.

The DFT computed conceptual density functional values suggest the increasing stability order of the tin(IV)porphyrin dihalides as **4 < 3 < 2 < 1.** They also suggest the more stable nature of the chloro (**2**) and fluoro (**1**) derivatives when compared to those of bromo (**3**) and iodo (**4**) compounds.

Bonding analysis of the frontier molecular orbitals suggests that in the HOMO, the delocalization of the electrons and orbital contribution from the porphyrin ring in compounds **1-3,** whereas HOMO of compound **4** is mainly from the halogen atom.

The Mayer bond analysis (MBA) predicts that the compounds (**1** & **2**) have bond order values of 0.4239, 0.6948 at Sn-N bonds. Also, the Sn-X bonds have better bonding interaction in compounds (3 & 4) with 1.1739 and 1.3679 bond orders.

DFT (BP86/TZVP) computed ^{1}H, ^{13}C, and ^{119}Sn NMR chemical shift values are in good agreement with those of the related similar tetraphenylporphyrinato compound. The ^{119}Sn chemical shift value of -58.72 ppm at upfield is in accordance with the highly shielded tin environment.

Funding

This research received no external funding.

Acknowledgments

Declared none.

Conflicts of Interest

The authors declare no conflict of interest.

References

1. Arnold, D.P.; Blok, J. The coordination chemistry of tin porphyrin complexes. *Coord. Chem. Rev.* **2004**, *248*, 299-319, https://doi.org/10.1016/j.ccr.2004.01.004.
2. Chandra, R.; Tiwari, M.; Kaur, P., Sharma, M.; Jain, R.; Dass, S. Metalloporphyrins-Applications and clinical significance. *Indian J. Clin. Biochem.* **2000**, *15*, 183-199, https://doi.org/10.1007/BF02867558.
3. Ghiggino, K.P.; Giri, N.K.; Hanrieder, J.; Martell, J.D.; Muller, J.; Paige, M.F.; Robotham, B.; Szmytkowski, J.; Steer, R.P. Photophysics of Soret-Excited Tin(IV) Porphyrins in Solution. *J. Phys. Chem. A* **2013**, *117*, 7833-7840, https://doi.org/10.1021/jp406025j.
4. Duan, M. Y.; Li, J.; Mele, G.; Wang, C.; Lu, X, F.; Vasapollo, G,; Zhang, F. X. Photocatalytic Activity of Novel Tin Porphyrin/TiO_2 Based Composites. *J. Phys. Chem. C* **2010**, *114*, 7857-7862, https://doi.org/10.1021/jp911744a.
5. Chaturvedi, A.; McCarver, G.A.; Sinha, S.; Hix, E.G.; Vogiatzis, K.D.; Jiang, J. A PEGylated Tin Porphyrin Complex for Electrocatalytic Proton Reduction: Mechanistic Insights into Main-Group-Element Catalysis. *Angew. Chem. Int. Ed.* **2022**, *61*, e202206325, https://doi.org/10.1002/anie.202206325.
6. Guenet, A.; Graf, E.; Kyritsakas, N.; Hosseini. M.W. Design and Synthesis of Sn-Porphyrin Based Molecular Gates. *Inorg. Chem.* **2010**, *49*, 1872-1883, https://doi.org/10.1021/ic902265e.
7. Dixon, D.W.; Schinazi, R.; Marzilli, L.G. Porphyrins as Agents against the Human Immunodeficiency Virus. *Ann. N. Y. Acad. Sci.* **1990**, *616*, 511-513, https://doi.org/10.1111/j.1749-6632.1990.tb17878.x.
8. Asanaka, M.; Kurimura, T.; Toya, H.; Ogaki, J.; Kato, Y. Sir, Anti-HIV activity of protoporphyrin. *AIDS* **1989**, *3*, 403, https://doi.org/10.1097/00002030-198906000-00014.
9. Hambright, P. Chemistry of Water Soluble Porphyrins. In The Porphyrin Handbook, Kadish, K.M.; Smith, K.M.; Guilard, R., Eds.; Elsevier, Academic Press, **2000**, Volume 3, 129-210.
10. Kumar, A.A.; Giribabu, L.; Reddy, R.D.; Maiya, B.G. New Molecular Arrays Based on a Tin(IV) Porphyrin Scaffold. *Inorg. Chem*. **2001**, *40*, 6757-6766, https://doi.org/10.1021/ic010179u.
11. Ravikumar, M.; Kathiravan, A.; Neels, A.; Mothi, E.M. Tin(IV) Porphyrins Containing β-Substituted Bromines: Synthesis, Conformations, Electrochemistry and Photophysical Evaluation. *Eur. J. Inorg. Chem.* **2018**, *2018*, 3868-3877, https://doi.org/10.1002/ejic.201800645.
12. Manke, A.-M.; Geisel, K.; Fetzer, A.; Kurz, P. A water-soluble tin(iv) porphyrin as a bioinspired photosensitiser for light-driven proton-reduction. *Phys. Chem. Chem. Phys.* **2014**, *16*, 12029-12042, https://doi.org/10.1039/C3CP55023K.
13. Kim, S.H.; Kim, H.; Kim, K.; Kim, H.-J. The first tin(IV) porphyrin complex with chiral amino acid ligands: synthesis, characterization and X-ray crystal structure of *trans*-bis(L-prolinato)[5,10,15,20-tetrakis-(4-

pyridyl)porphyrinato]tin(IV). *J. Porphyr. Phthalocyanines* **2009**, *13*, 805-810, https://doi.org/10.1142/S108842460900098X.
14. Agnihotri, N.; Steer, R.P. TD-DFT calculations of the excited states of metalloporphyrins relevant to organic solar photovoltaic cells. *J. Porphyr. Phthalocyanines* **2014**, *18*, 475-492, https://doi.org/10.1142/S1088424614500230.
15. Leu, B.M.; Zgierski, M.Z.; Bischoff, C.; Li, M.; Hu, M.Y.; Zhao, J.; Martin, S.W.; Alp, E.E.; Scheidt, W.R. Quantitative Vibrational Dynamics of the Metal Site in a Tin Porphyrin: An IR, NRVS, and DFT Study. *Inorg. Chem.* **2013**, *52*, 9948-9953, https://doi.org/10.1021/ic401152b.
16. Li, L.; Li, H.; Shi, L.; Shi, L.; Li, T. Tin Porphyrin-Based Nanozymes with Unprecedented Superoxide Dismutase-Mimicking Activities. *Langmuir* **2022**, *38*, 7272-7279, https://doi.org/10.1021/acs.langmuir.2c00778.
17. Drummond, G.S.; Kappas, A. Chemoprevention of Neonatal Jaundice: Potency of Tin-Protoporphyrin in an Animal Model. *Science* **1982**, *217*, 1250-1252, https://doi.org/10.1126/science.6896768.
18. Thomas, A.; Kuttassery, F.; Remello, S.N.; Mathew, S.; Yamamoto, D.; Onuki, S.; Nabetani, Y.; Tachibana, H.; Inoue, H. Facile Synthesis of Water-Soluble Cationic Tin(IV) Porphyrins and Water-Insoluble Tin(IV) Porphyrins in Water at Ambient Temperature. *Bull. Chem. Soc. Jpn.* **2016**, *89*, 902-904, https://doi.org/10.1246/bcsj.20160091.
19. Huang, H.; Chauhan, S.; Geng, J.; Qin, Y.; Watson, D.F.; Lovell, J.F. Implantable Tin Porphyrin-PEG Hydrogels with pH-Responsive Fluorescence. *Biomacromolecules* **2017**, *18*, 562-567, https://doi.org/10.1021/acs.biomac.6b01715.
20. Patel, T.R.; Ganguly, B. Exploring the metal-free catalytic reduction of CO_2 to methanol with saturated adamantane scaffolds of phosphine-borane frustrated Lewis pair: A DFT study. *J. Mol. Graph. Model.* **2022**, *113*, 108150, https://doi.org/10.1016/j.jmgm.2022.108150.
21. Neese, F. Software update: The ORCA program system—Version 5.0. *WIREs Comput. Mol. Sci*. **2022**, *12*, e1606, https://doi.org/10.1002/wcms.1606.
22. Vosko, S.H.; Wilk, L.; Nusair, M. Accurate spin-dependent electron liquid correlation energies for local spin density calculations: a critical analysis. *Can. J. Phys*. **1980**, *58*, 1200-1211, http://doi.org/10.1139/p80-159.
23. Becke, A.D. Density functional calculations of molecular bond energies. *J. Chem. Phys*. **1986**, *84*, 4524-4529, https://doi.org/10.1063/1.450025.
24. Becke, A.D. Density-functional exchange-energy approximation with correct asymptotic behavior. *Phys. Rev. A* **1988**, *38*, 3098, https://doi.org/10.1103/PhysRevA.38.3098.
25. Perdew, J.P. Density-functional approximation for the correlation energy of the inhomogeneous electron gas. *Phys. Rev. B*, **1986**, *33*, 8822, https://doi.org/10.1103/PhysRevB.33.8822.
26. Weigend, F.; Ahlrichs, R. Balanced basis sets of split valence, triple zeta valence and quadruple zeta valence quality for H to Rn: Design and assessment of accuracy. *Phys. Chem. Chem. Phys.* **2005**, *7*, 3297-3305, https://doi.org/10.1039/b508541a.
27. Reveles, J.U.; Köster, A.M. Geometry optimization in density functional methods. *J. Comput. Chem.* **2004**, *25*, 1109 –1116, https://doi.org/10.1002/jcc.20034.
28. Schlegel, H.B. Geometry optimization. *WIREs Comput. Mol. Sci.* **2011**, *1*, 790–809, https://doi.org/10.1002/wcms.34.
29. Mareš, J.; Vaara, J. *Ab initio* paramagnetic NMR shifts *via* point-dipole approximation in a large magnetic-anisotropy Co(II) complex. *Phys. Chem. Chem. Phys.* **2018**, *20*, 22547-22555, https://doi.org/10.1039/C8CP04123G.
30. Becker, E.D. Chapter 4 - Chemical Shifts. In High Resolution NMR (Third Edition), Academic Press, **2000**, 83-117, https://doi.org/10.1016/B978-012084662-7/50048-X.
31. Guzman, A.L.; Hoye, T.R. TMS is Superior to Residual C*H*Cl_3 for Use as the Internal Reference for Routine ^{1}H NMR Spectra Recorded in $CDCl_3$. *J. Org. Chem.* **2022**, *87*, 905–909, https://doi.org/10.1021/acs.joc.1c02590.
32. Oller, J.; Pérez, P.; Ayers, P.W.; Vöhringer-Martinez, E. Global and local reactivity descriptors based on quadratic and linear energy models for *α*,*β*-unsaturated organic compounds. *Int. J. Quantum. Chem.* **2018**, *118*, e25706, https://doi.org/10.1002/qua.25706.
33. Giannoudis, E.; Benazzi, E.; Karlsson, J.; Copley, G.; Panagiotakis, S.; Landrou, G.; Angaridis, P.; Nikolaou, V.; Matthaiaki, C.; Charalambidis, G.; Gibson, E.A.; Coutsolelos, A.G. Photosensitizers for H_2

Evolution Based on Charged or Neutral Zn and Sn Porphyrins. *Inorg. Chem.* **2020**, *59*, 1611–1621, https://doi.org/10.1021/acs.inorgchem.9b01838.

34. Khan, R.; Tariq, M.; Shah, K.H.; Rani, S.; Osman, N.A.; Asif, H.M; Mehar, S.; Alanazi, A.K.; Abo-Dief, H.M. Covalent synthesis, structural characterization and biological behavioral study of tin captured porphyrin-polyoxometalate based polymeric hybrid. *J. Photochem. Photobiol. A Chem.* **2023**, *442*, 114774, https://doi.org/10.1016/j.jphotochem.2023.114774.
35. Poudel, P.; Adhikari, S. Efficacy and Safety Concerns with Sn-Mesoporphyrin as an Adjunct Therapy in Neonatal Hyperbilirubinemia: A Literature Review. *Int. J. Pediatr.* **2022**, *2022*, 2549161, https://doi.org/10.1155/2022/2549161.
36. Rosenfeld, W.N.; Hudak, M.L.; Ruiz, N.; Gautam, S.; The Jasmine Study Group. Stannsoporfin with phototherapy to treat hyperbilirubinemia in newborn hemolytic disease. *J. Perinatol.* **2022**, *42*, 110–115, https://doi.org/10.1038/s41372-021-01223-2.
37. Karpova, S.G.; Ol'khov, A.A.; Zhul'kina, A.L.; Popov, A.A.; Iordanskii, A.L. Nonwoven Materials Based on Electrospun Ultrathin Fibers of Poly(3-hydroxybutyrate) and Complex Tin Chloride–Porphyrin. *Polym. Sci. Ser. A* **2021**, *63*, 369–381, https://doi.org/10.1134/S0965545X21040040.
38. Stadlbauer, S.; Grössl, D.; Fischer, R.; Demitri, N.; Uhlig, F. Redistribution reaction on a six-fold coordinated Sn(IV) atom and reactions towards axially unsymmetric substituted Sn(IV) porphyrins. *J. Organomet. Chem.* **2020**, *925*,121470, https://doi.org/10.1016/j.jorganchem.2020.121470.
39. Thomas, A.; Ohsaki, Y.; Nakazato, R.; Kuttassery, F.; Mathew, S.; Remello, S.N.; Tachibana, H.; Inoue, H. Molecular Characteristics of Water-Insoluble Tin-Porphyrins for Designing the One-Photon-Induced Two-Electron Oxidation of Water in Artificial Photosynthesis. *Molecules* **2023**, *28*, 1882, https://doi.org/10.3390/molecules28041882.
40. Yasmeen, R.; Singhaal, R.; Bajju, G.D.; Sheikh, H.N. Axially coordinated tin porphyrins anchored graphene oxide hybrid composites as productive catalyst for catalytic conversion of 4-nitrophenol to 4-aminophenol. *J. Chem. Sci.* **2022**, *134*, 111, https://doi.org/10.1007/s12039-022-02105-6.